universe

MDPI

Article

Strong Deflection Gravitational Lensing for the Photons Coupled to the Weyl Tensor in a Conformal Gravity Black Hole

Ghulam Abbas [1,*], Ali Övgün [2], Asif Mahmood [1] and Muhammad Zubair [3]

[1] Department of Mathematics, The Islamia University of Bahawalpur, Bahawalpur 63100, Pakistan
[2] Physics Department, Eastern Mediterranean University, North Cyprus via Mersin 10, Famagusta 99628, Turkey
[3] Department of Mathematics, COMSATS University Islamabad, Lahore Campus, Lahore 45550, Pakistan
* Correspondence: abbasg91@yahoo.com

Abstract: In the present paper, strong deflection gravitational lensing is studied in a conformal gravity black hole. With the help of geometric optics limits, we have formulated the light cone conditions for the photons coupled to the Weyl tensor in a conformal gravity black hole. It is explicitly found that strong deflection gravitational lensing depends on the coupling with the Weyl tensor, the polarization directions, and the black hole configuration parameters. We have applied the results of the strong deflection gravitational lensing to the supermassive black holes $SgrA^*$ and $M87^*$ and studied the possibility of encountering quantum improvement. It is not practicable to recognize similar black holes through the strong deflection gravitational lensing observables in the near future, except for the possible size of the black hole's shadow. We also notice that by directly adopting the constraint of the measured shadow of $M87^*$, the quantum effect demands immense care.

Keywords: strong deflection gravitational lensing; conformal gravity; black hole physics

check for updates

Citation: Abbas, G.; Övgün, A.; Mahmood, A.; Zubair, M. Strong Deflection Gravitational Lensing for the Photons Coupled to the Weyl Tensor in a Conformal Gravity Black Hole. *Universe* **2023**, *9*, 130. https://doi.org/10.3390/universe9030130

Academic Editor: Lorenzo Iorio

Received: 31 January 2023
Revised: 25 February 2023
Accepted: 26 February 2023
Published: 2 March 2023

Copyright: © 2023 by the authors. Licensee MDPI, Basel, Switzerland. This article is an open access article distributed under the terms and conditions of the Creative Commons Attribution (CC BY) license (https://creativecommons.org/licenses/by/4.0/).

1. Introduction

Conformal (Weyl) gravity is a curious gravitational theory in four dimensions defined through the action provided by the Weyl tensor square, where $S_{conf} = \int d^4x\sqrt{g}W^2$. The Weyl's transformation of the metric ($g_{\alpha\beta} \to \Omega^2(x)g_{\alpha\beta}$) is a specific symmetry of that action. This theory has appeared periodically for many causes. It was studied as a desirable UV culmination of gravity [1–3] and also for the useful setting up of supergravity theories [4,5] as a result of twistor string theory [6]. Recently, conformal (Weyl) gravity, formulated by Weyl's pure square action, has been considered a good substitute for Einstein's gravity. From the symmetry of conformal gravity and the equation of motion, the conformal solution to Einstein field equations emerges naturally as a solution to conformal gravity. Basically, depending on the state of the Neumann boundary, gravity may agree with Einstein's solution [7,8]. Moreover, in contrast to Einstein's gravity, conformal gravity has been proven to be repetitive in terms of four dimensions [9], resulting in exciting forms of quantum gravity [10]. Another interesting feature of conformal gravity arises from cosmology. Though Einstein's gravity can fully explain the physics at a solar system scale, there are some unresolved issues when considering large scales, which include incompatibility detection of galactic curves and accelerating space. As a result, anonymous organizations that are "dark matter and dark energy" should be introduced to address these problems of non-compliance. Therefore, one may think of the possibilities for changing the state of gravity for the explanation of physics at larger scales while preserving the right character at the solar system scale. Moreover, conformal gravity allows for more solutions than Einstein's, which can yield effective energy in tandem with this visual object, making it an attractive gravitational view [3,11–14]. Conformal gravity as well as Einstein's gravity can share similar solutions of spacetime, and a black hole's thermodynamic quantities, such as the mass and entropy, depend on the action instead of the line element.

The difference in action can be explained by how the thermodynamics of black holes for two different magnetic fields can vary. The thermodynamical phase structure of this conformal gravity in 4D (A)dS black hole spacetime was examined [15–18]. The formation of a conformal gravity contains two types of equations for statistics. One is a zero-order phase transformation, while the other is a Hawking Page-like transformation. Now, we give a brief review of gravitational lensing, which occurs due to the bending of light rays when they pass nearby the massive object [19] and the object produces a noticeable deviation, termed a gravitational lens. Now, this strong deflection (SD) lensing phenomenon has been proven to be a major tool for detecting the existence of gravitational waves and black holes in the cosmos [20]. In 1959, for the first time, it was predicted by Darwin [21] that the light emitted by a large deviation could prevent many loops before its escape when light rays pass too close to astrophysical structures such as black holes, and reliable images appear on all sides of the object. In addition, the information contained in the photographs involved can be useful in the study of the properties of massive objects in the cosmos. This research could play a significant role in studying other theories of gravity in its strongest deviation field [22–32]. Eiroa [33] explored the physical profiles of photons in Born–Infeld electrodynamics and pointed out that the geodesics method depends on the Born–Infeld combination. The nature of gravity is widely discussed in many theories of gravity [34–42], and it has been proven to be a major aspect of celestial bodies. It is known that the dynamic force of gravity depends on the formation of the curvature of the background, the powerful features of photons, and the interaction of light with various other fields. Actually, light is considered to be a type of electric wave. The distribution of photons will be altered due to the coupling between the electromagnetic tensors and the curvature, resulting in some incidents of SD gravitational lensing.

Drummond [43] found that the effective action of photons is achieved by single-loop vacuum polarization when a similar kind of coupling is applied in quantum electrodynamics (QED). By considering the effective field theory, the coupling of the electromagnetic field and the Riemann curvature tensors is considered to be quantum, and hence all the combined terms remain small. Thus, the combined terms must have values of the second order of the Compton wavelength of the electron $\tilde{\lambda}_e$. Turner [44] found more interesting results than the electromagnetic variation by rethinking the Drummond model [43] with the coupling combination. Ni [45,46] presented a generalized electrical model and proved that the electrical power with the Riemann curvature tensor is often combined at the intervals of integration. Ni's electric model [45,46] has been discussed extensively [47–53]. Such kinds of model have been thoroughly studied for the specific selection of constants in [44–61] for the cause of further physical attraction. Ritz and Ward [62] showed that the electric power of Weyl's adjustment and the global relationship with the average payout of U(1) has a changing holographic conduction after the (A)dS space period. The value of the critical temperature and the order of the phase are altered in the origination of holographic superconductors [63–70]. The powerful evolution and the Hawking radiations for electromagnetism have dependence on the integration parameter of the field [71–75].

The authors of [76,77] measured the weak as well as SD gravitational lensing that removes the gravity of photons attached to the Weyl tensor and found the SD angle, the angular separation, and the brightness variation among the relativistic picture outcomes. Moreover, the time delay among such types of interlinked images was also found in [78,79]. Among these, gravitational lensing in the weak or strong gravity regime of a black hole has gained a lot of attention since it can reveal a black hole's features [80–95]. For instance, Horvath et al. studied gravitational lensing in the Kehagias–Sfetsos spacetime emerging in the framework of Hořava–Lifshitz gravity [80]. Eiroa and Sendra studied gravitational lensing by braneworld black holes with no matter or mass [81]. Moreover, Izmailov et al. investigated light deflection in modified gravity in the weak and strong field regimes [82]. Weak and strong deflection gravitational lensing by the hairy black holes in Einstein-scalar Gauss–Bonnet gravity with five types of coupling functions (quadratic, cubic, quartic, inverse-polynomial, and logarithmic), which can evade the no-hair theorem, were stud-

ied by Gao and Xie [83]. Cheng and Xie [84] showed that the black bounce traversable wormhole is indistinguishable from a Schwarzschild black hole and is loosely tested by the Event Horizon Telescope in strong deflection gravitational lensing. In addition, Zhang and Xie studied weak and strong deflection gravitational lensing with a black bounce Reissner–Nordström spacetime and obtained their lensing observables [85].

Li [96,97] proposed the old photon tests integrated with the Weyl tensor for the solar system. Pang [98] explored the gravitational lensing of massless and giant particles in a Reissner–Nordström (RN) black hole. Tsukamoto [99] calculated the SD angle in the static, spherically symmetric, and asymptotically flat spacetime. Eiroa [32] investigated the SD gravitational lensing phenomenon by taking an RN black hole as a lens and worked on the positions and magnifications of these relativistic images. Zakharov [100] explored the direct measurements of a black hole's charge with future astrometrical missions. Moreover, weak and SD gravitational lensing by a charged Horndeski [101] and renormalization group-improved Schwarzschild black hole [102] were investigated. The phenomenon of SD gravitational lensing was investigated through several black holes, including braneworld black holes [103], a charged Galileon black hole [104], and a modified Hayward black hole [105]. More work concerning SD gravitational lensing has been performed for different black hole spacetimes, such as a Kerr black hole [106], a regular phantom black hole [107], a Kiselev black hole [108], and a charged Kiselev black hole [109]. All the considered black holes for SD gravitational lensing are asymptotically flat. It would be interesting to study the SD gravitational lensing for a non-asymptotically flat black hole, such as a conformal gravity black hole, which is non-asymptotically flat due to terms proportional to r and r^2.

Aside from the requirement for dark matter in galaxies, the standard Newton–Einstein theory also calls for more dark matter in clusters of galaxies than is contained within the individual galaxies within the cluster. This fact is also qualitatively consistent with the conformal theory, because the linear potential term leads to larger and larger deviations from the standard theory at larger and larger distance scales. Galactic gravitational lensing provides an actual possible comparative test of the relative merits of the conformal theory and the standard dark matter scenario, which might even be demonstrated to be conclusive once a detailed picture of gravitational lensing is calculated in a fourth-order theory, such as the Weyl theory of gravity. Thus far, all considered black holes for SD gravitational lensing have been asymptotically flat. It would be interesting to study SD gravitational lensing for a non-asymptotically flat black hole, such as a conformal gravity black hole, which is non-asymptotically flat due to a term proportional to r [110].

In this work, the SD gravitational lensing phenomenon is explored for the photons coupled to the Weyl tensor in a conformal gravity black hole. In addition, we study the consequences of coupling on the motion of the photon sphere, the SD angle, and the SD gravitational lensing observables for $SgrA^*$ and $M87^*$. This paper is ordered as follows. In Section 2, the equations of motion are investigated for the photons coupled to the Weyl tensor in conformal gravity. In Sections 3 and 4, the photon sphere equation, the SD angle, and the SD gravitational lensing observables for $SgrA^*$ and $M87^*$ are probed. In the last section, we give our outcomes.

2. Conformal Gravity Black Hole

The electromagnetic field action for the photons coupled to the Weyl tensor [62,76,78,97,106,108,109] is given by

$$S = \int d^4x\sqrt{-g}[\frac{R}{16\pi G} - \frac{1}{4}(F_{\alpha\beta}F^{\alpha\beta} - 4\tilde{\alpha}C_{\alpha\beta\mu\nu}F^{\alpha\beta}F^{\mu\nu})], \quad (1)$$

where $F_{\alpha\beta} = \nabla_\alpha A_\beta - \nabla_\beta A_\alpha$ denotes the electromagnetic field tensor, A_α represents the gauge potential, and $\tilde{\alpha}$ is a coupling parameter. Other terms such as R and $C_{\alpha\beta\mu\nu}$ repre-

sent the Ricci scalar and the Weyl tensor, respectively. For any n dimensional spacetime, $C_{\alpha\beta\mu\nu}$ [76] is defined as follows:

$$C_{\alpha\beta\mu\nu} = R_{\alpha\beta\mu\nu} - \frac{2}{n-2}(g_{\alpha[\mu}R_{\nu]\beta} - g_{\beta[\mu}R_{\nu]\alpha}) + \frac{2}{(n-1)(n-2)}Rg_{\alpha[\mu}g_{\nu]\beta}. \quad (2)$$

The simplest form of the four-dimensional conformal gravity black hole [111–113] is defined by

$$ds^2 = g(r)dr^2 + r^2(d\theta^2 + \sin^2\theta d\phi^2) - f(r)dt^2\,, \quad (3)$$

with

$$f(r) = c_0 + c_1 r + \frac{d}{r} - \frac{1}{3}\Lambda r^2, \quad (4)$$

and $g(r) = f^{-1}(r)$. The four integral constants c_0, c_1, d, and Λ can be defined under the given constraint [113]

$$c_0^2 = 3c_1 d + 1, \quad (5)$$

which implies

$$c_0 = \pm\sqrt{3c_1 d + 1}\,. \quad (6)$$

If we take $c_1 = 0$ and $c_0 = 1$, then the solution reduces to the Schwarzschild (A)dS black hole. The last term of Equation (4) contains Λ, which corresponds to the"cosmological constant" that comes from the integral rather than the action. The electromagnetic field action in Equation (1) with (A_α) gives the following corrected Maxwell equation [76]:

$$\nabla_\alpha(F_{\alpha\beta} - 4\tilde{\alpha}C_{\alpha\beta\mu\nu}F^{\mu\nu}) = 0, \quad (7)$$

which means that the photons' propagation will change via the Weyl tensor, and the wavelength of the coupled photons is greater than the electron Compton wavelength, but it is smaller than the traditional curvature scale (i.e., $\tilde{\lambda_e} < \tilde{\lambda_p} < \tilde{\mathfrak{L}}$). This signifies that both the electromagnetic and gravitational fields may be neglected by the typical curvature scale for the coupled photon propagation. Now, by using the geometric optics approximations [43,114–119], we can easily find the electromagnetic field tensor [76]:

$$F_{\alpha\beta} = f_{\alpha\beta}e^{\mu\theta}\,. \quad (8)$$

The term $f_{\alpha\beta} = k_\alpha a_\beta - k_\beta a_\alpha$ and the quantity θ are the slowly varying amplitude and rapidly varying parameter, respectively. Here, a_α defines the polarization vector satisfying the condition $k^\alpha a_\alpha = 0$, and k_α represents the wave vector (i.e., $k_\alpha = \partial_\alpha\theta$). The derivative term $f_{\alpha\beta;\lambda}$ can be omitted. Now, by solving Equations (7) and (8), we can find the equation of motion for the photons coupled to $C_{\alpha\beta\mu\nu}$:

$$k^\alpha k_\alpha a_\beta + 8\tilde{\alpha}C_{\alpha\beta\mu\nu}k^\alpha k^\mu a^\nu = 0. \quad (9)$$

Now, we introduce the field of tetrads (vierbeins) as follows [76]:

$$g_{\alpha\beta} = \eta_{\mu\nu}e^\mu_\alpha e^\nu_\beta, \quad (10)$$

and

$$e^\mu_\alpha = \mathrm{diag}(\sqrt{f(r)}\,,\ \sqrt{g(r)}\,,\ \sqrt{h(r)}\,,\ \sqrt{h(r)}\,\sin\theta)\,. \quad (11)$$

In Equation (10), $\eta_{\mu\nu}$ defines the Minkowski metric, and $e^\mu_\alpha, e^\nu_\beta$ are called vierbeins. The vierbeins in the form of an antisymmetric combination may be expressed as [43,114–116] $U^{\mu\nu}_{\alpha\beta} = e^\mu_\alpha e^\nu_\beta - e^\mu_\beta e^\nu_\alpha$. The complete Weyl tensor $C_{\alpha\beta\mu\nu}$ can be rewritten as follows [76]:

$$C_{\alpha\beta\mu\nu} = \mathcal{A}(2U^{12}_{\alpha\beta}U^{12}_{\mu\nu} - U^{13}_{\alpha\beta}U^{13}_{\mu\nu} - U^{14}_{\alpha\beta}U^{14}_{\mu\nu} + U^{23}_{\alpha\beta}U^{23}_{\mu\nu} + U^{24}_{\alpha\beta}U^{24}_{\mu\nu} - 2U^{34}_{\alpha\beta}U^{34}_{\mu\nu}), \quad (12)$$

where

$$\mathcal{A} = -\frac{1}{12r^2}[r^2 f''(r) - 2rf'(r) + 2f(r) - 2]. \tag{13}$$

Here, we introduce the three combinations of momentum components [43,114–116] (i.e., $l_\beta = k^\alpha U^{12}_{\alpha\beta}$, $n_\beta = k^\alpha U^{13}_{\alpha\beta}$, and $m_\beta = k^\alpha U^{34}_{\alpha\beta}$). After a tedious calculation, Equation (9) provides the precise light cone conditions [76]:

$$g^{11}k_1k_1 + g^{22}k_2k_2 + g^{33}k_3k_3 + g^{44}k_4k_4 = 0\,, \tag{14}$$

with

$$g^{11} = -(e^t_1)^2, \quad g^{22} = (e^r_2)^2, \quad g^{33} = (e^\theta_3)^2\, W(r), \quad g^{44} = (e^\phi_4)^2\, W(r). \tag{15}$$

Here, we have

$$W(r) = \frac{3r^3 + 12\tilde{\alpha}d - 4\tilde{\alpha}r + 4\tilde{\alpha}c_0 r}{3r^3 - 24\tilde{\alpha}d + 8\tilde{\alpha}r - 8\tilde{\alpha}c_0 r}\,. \tag{16}$$

and

$$W(r) = \frac{3r^3 - 24\tilde{\alpha}d + 8\tilde{\alpha}r - 8\tilde{\alpha}c_0 r}{3r^3 + 12\tilde{\alpha}d - 4\tilde{\alpha}r + 4\tilde{\alpha}c_0 r}\,, \tag{17}$$

The variable $W(r)$ depends on the coupled photon polarization. Therefore, Equation (16) is analogous to the coupled photon polarization along l_α for PPL, and Equation (17) is analogous to the coupled photon polarization along m_α for PPM.

3. Equation of the Photon Sphere

The effective metric $\gamma_{\alpha\beta}$ (i.e., $\gamma^{\alpha\beta}k_\alpha k_\beta = 0$) in a conformal gravity black hole is defined as follows [76,120]:

$$ds^2 = B(x)dx^2 + C(x)W^{-1}(x)d\theta^2 + C(x)W^{-1}(x)\sin^2\theta d\phi^2 - A(x)dt^2, \tag{18}$$

and

$$A(x) = B^{-1}(x) = c_0 + c_1 x + \frac{d}{x} - \frac{1}{3}\Lambda x^2, \tag{19}$$

$$C(x) = x^2, \tag{20}$$

$$W(x) = \frac{3x^3 + 12\tilde{\alpha}d - 4\tilde{\alpha}x + 4\tilde{\alpha}c_0 x}{3x^3 - 24\tilde{\alpha}d + 8\tilde{\alpha}x - 8\tilde{\alpha}c_0 x} \qquad \text{for PPL,} \tag{21}$$

$$W(x) = \frac{3x^3 - 24\tilde{\alpha}d + 8\tilde{\alpha}x - 8\tilde{\alpha}c_0 x}{3x^3 + 12\tilde{\alpha}d - 4\tilde{\alpha}x + 4\tilde{\alpha}c_0 x} \qquad \text{for PPM.} \tag{22}$$

By using the symmetry of the black hole, we can obtain the geodesic constants of motion [76]:

$$E = \frac{dt}{d\lambda}\,, \qquad L = \frac{d\phi}{d\lambda}A(x)\,C(x)\,W^{-1}(x). \tag{23}$$

The parameter E stands for the energy, and L stands for the angular momentum per unit mass, while λ is called the affine parameter. Moreover, it is found that the photons obtain various trajectories with various polarizations, and hence every side of the bodies has two sets of relativistic images, since the observer as well as the source are placed in the required equatorial plane (i.e., $\theta = 90^\circ$). With Equation (23), and using the condition $k_\alpha = g_{\alpha\beta}\frac{dx^\beta}{d\lambda}$, we see that Equation (9) for the photons in the conformal gravity BH can be further rewritten as follows:

$$(\frac{dx}{d\lambda})^2 = A(x)\left(\frac{E^2}{A(x)} - W(x)\frac{L^2}{C(x)}\right). \tag{24}$$

Now, by studying the photon sphere equation [22,121,122], it is easy to find the impact parameter and the equation of the photon sphere [76] in this scenario:

$$u(x) = \frac{\sqrt{C(x)}}{\sqrt{A(x)W(x)}}, \tag{25}$$

and

$$A(x)C(x)W'(x) + [A'(x)C(x) - A(x)C'(x)]W(x) = 0. \tag{26}$$

Here, the sign $'$ represents the radial derivatives. Here, the photon sphere is described as the innermost circulating orbit for the photons. If we find the solution to Equation (26), then the radius of the photon sphere appears as its largest root. We study the radius x_{ps} with $\tilde{\alpha}$ (coupling parameter) and c_1 (black hole parameter) for the PPL and PPM cases (see Figure 1). This shows that when $\tilde{\alpha}$ increases with c_1, the radius becomes $x_{ps} = 1.9$ for PPL and $x_{ps} = 2.85$ for PPM. It is easy to find that $\tilde{\alpha}$ is a constant with the length-squared dimension, and in order to be consistent with the observation, we have to constrain $\tilde{\alpha} \leq 10^{13} m^2$ [96]. If we take the the BHs in the galactic center as $SgrA^*$ having a mass $M = 4.28 \times 10^6 M_\odot$ [123] and $M87^*$ having a mass $m_\bullet = 6.5 \times 10^9 M_\odot$ [124], then the dimensionless coupling constant $\tilde{\alpha} \sim 10^{-7}$. The same procedure was adopted in [107] to discuss the strong gravitational lensing for photons coupled to the Weyl tensor in a regular phantom BH.

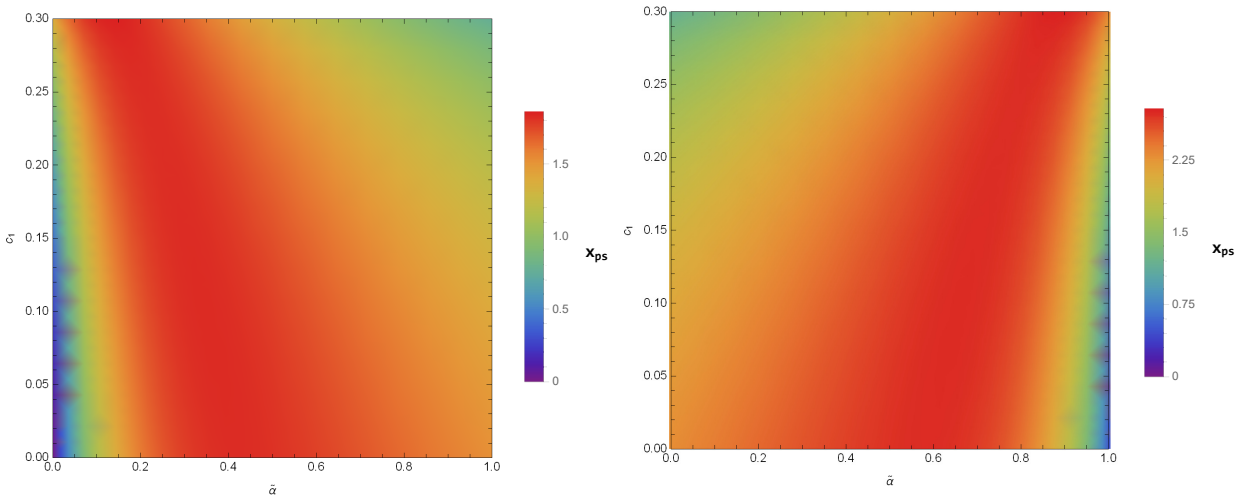

Figure 1. Color-indexed variations of the radius (x_{ps}) with $\tilde{\alpha}$ and c_1 (**left**) for PPL and (**right**) for PPM. Here, we set $c_0 = \sqrt{3c_1 d + 1}$, $d = 1$, and $\Lambda = -1$.

4. Strong Deflection Angle

In this part, we study the SD angle as the null geodesic (i.e., the photons coming from infinity) become limited. Hence, the SD angle can be defined as [125]

$$\alpha(x_0) = I(x_0) - \pi, \tag{27}$$

and

$$I(x_0) = 2\int_{x_0}^{\infty} \frac{dx}{\sqrt{\frac{A(x)C(x)}{W(x)}}\sqrt{\frac{A(x_0)C(x)W(x_0)}{A(x)C(x_0)W(x)} - 1}}. \tag{28}$$

The variable x_0 stands for the closest approach distance. We see that as $x_0 \to x_{ps}$, the SD angle $\alpha(x_0)$ diverges while the photons are caught from the black hole, which assures that certain light rays cause a complete loop about the heavy objects before arriving at the observer. Furthermore, as $\alpha(x_0)$ changes into 2π for a specific value of x_0, the SD angle increases, but the distance decreases. Hence, the physical characteristics of the SD angle are

perfectly various. By adopting the Bozza technique $z = 1 - \frac{x_0}{x}$ [27], Equation (28) further reduces to

$$I(x_0) = \int_0^1 F(z, x_0) R(z, x_0) dz, \tag{29}$$

where

$$R(z, x_0) = 2\frac{W(x)x^2\sqrt{C(x_0)}}{x_0 C(x)} = 2W(z, x_0), \tag{30}$$

$$F(z, x_0) = \frac{1}{\sqrt{W(x_0)A(x_0) - \frac{W(z,x_0)A(z,x_0)C(x_0)}{C(z,x_0)}}}. \tag{31}$$

The function $F(z, x_0)$ deviates as $z \to 0$, but the function $R(z, x_0)$ is regular for each value of x_0 and z . Now, we separate the integral in Equation (29) into two particular parts ($I_D(x_0)$, the divergent part, and $I_R(x_0)$, the regular part) as follows:

$$I_D(x_0) = \int_0^1 R(0, x_{ps}) F_0(z, x_0) dz. \tag{32}$$

and

$$I_R(x_0) = \int_0^1 [R(z, x_o) F(z, x_0) - R(0, x_{ps}) F_0(z, x_0)] dz. \tag{33}$$

The function $F_0(z, x_0)$ is described as follows:

$$F_0(z, x_0) = \frac{1}{\sqrt{f_1(x_0)z + f_2(x_0)z^2}}, \tag{34}$$

with

$$f_1(x_0) = \frac{x_0}{C(x_0)}\{W(x_0)[A(x_0)C'(x_0) - A'(x_0)C(x_0)] - A(x_0)C(x_0)W'(x_0)\}, \tag{35}$$

$$\begin{aligned} f_2(x_0) &= \frac{x_0}{2C^2(x_0)}\{2[C(x_0) - x_0C'(x_0)][A(x_0)W(x_0)C'(x_0) - C(x_0)(A(x_0)W(x_0))'] \\ &+ x_0C(x_0)[A(x_0)W(x_0)C''(x_0) - C(x_0)(A(x_0)W(x_0))'']\}. \end{aligned} \tag{36}$$

When $f_1(x_0)$ is nonzero ($x_0 \neq x_{ps}$), the dominant order of the divergence in $F_0(z, x_0)$ assumes the form of $\frac{1}{\sqrt{z}}$ but is integrated to give limited consequences. As $f_1(x_0)$ vanishes ($x_0 = x_{ps}$), the aforementioned result becomes $\frac{1}{z}$, which causes the integral to appear to be divergent. In this situation, every photon ($x_0 < x_{ps}$) is caught from the central body and cannot be brought back up. However, the SD angle diverges logarithmically for the photons [27]:

$$\alpha(\theta) = -\bar{a}\log[\frac{\theta D_{OL}}{u(x_{ps})} - 1] + \bar{b} + O[u(x) - u(x_{ps})]. \tag{37}$$

Here, we have

$$\begin{aligned} \bar{a} &= \frac{R(0, x_{ps})}{2\sqrt{f_2(x_{ps})}}, \\ b_R &= I_R(x_{ps}), \\ \bar{b} &= \bar{a}\log[\frac{2x_{hs}^2 u(x_{ps})''}{u(x_{ps})}] - \pi + b_R. \end{aligned} \tag{38}$$

Here, D_{OL} stands for the distance between the observer and the gravitational lens. From Equations (21) and (22), the numerical characteristic of $\alpha(\theta)$ in conformal gravity is studied. The variations of the quantities with bars ($\bar{a}$ and $\bar{b}$) for different values of $\tilde{\alpha}$ and c_1 are given in Figures 2 and 3. The coefficients $\bar{a}$ and $\bar{b}$ not only depend on the parameters of

the black hole but also on the coupling parameter and the polarization directions of the photons. Hence, with the increase in $\tilde{\alpha}$ and in the constant c_1, the coefficients $\bar{a}$ and $\bar{b}$ have values $\bar{a} = 1.25$ and $\bar{b} = 4.1$ for PPL and $\bar{a} = 1$ and $\bar{b} = 3.2$ for PPM. Since, the coefficients are the functions of $\tilde{\alpha}$, the alike features may be observed in the SD angle. We study the variations of $\alpha(\theta)$ calculated at $u = u_{ps} + 0.003$, presented in Figure 4, where it is noted that the SD angle ($\alpha(\theta)$) has the values $\alpha(\theta) = 5.75$ for PPL and $\alpha(\theta) = 4.75$ for PPM.

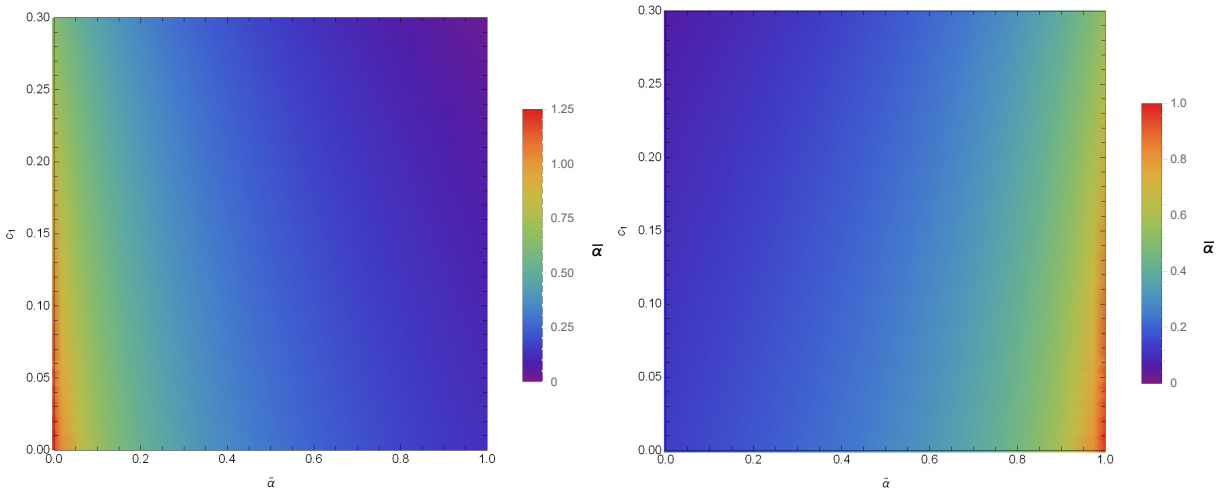

Figure 2. Color-indexed variations of the coefficient ($\bar{a}$) with $\tilde{\alpha}$ and c_1 (**left**) for PPL and (**right**) for PPM. Here, we set $c_0 = \sqrt{3c_1d + 1}$, $d = 1$, and $\Lambda = -1$.

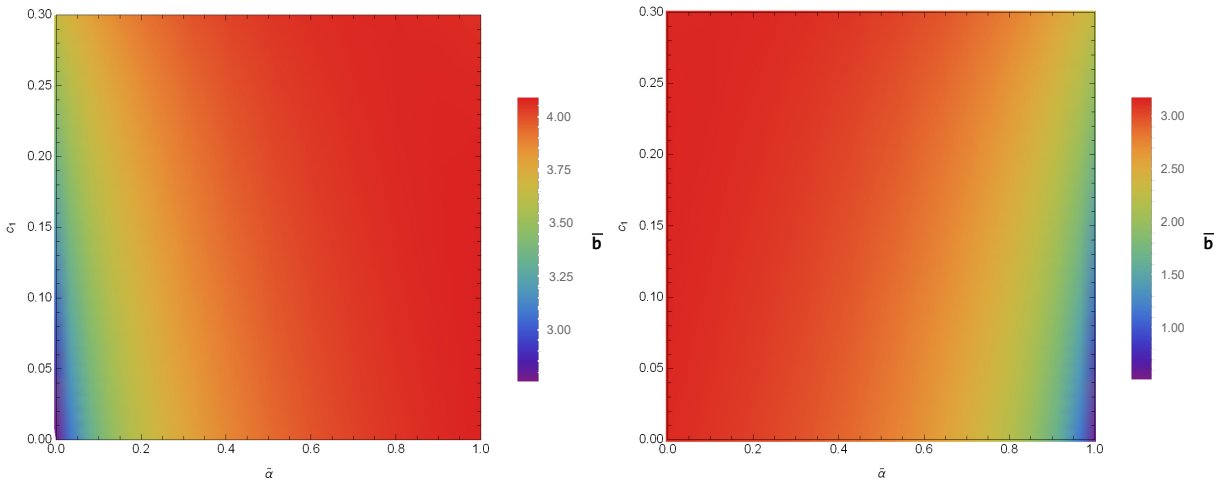

Figure 3. Color-indexed variations of the coefficient ($\bar{b}$) with $\tilde{\alpha}$ and c_1 (**left**) for PPL and (**right**) for PPM. Here, we set $c_0 = \sqrt{3c_1d + 1}$, $d = 1$, and $\Lambda = -1$.

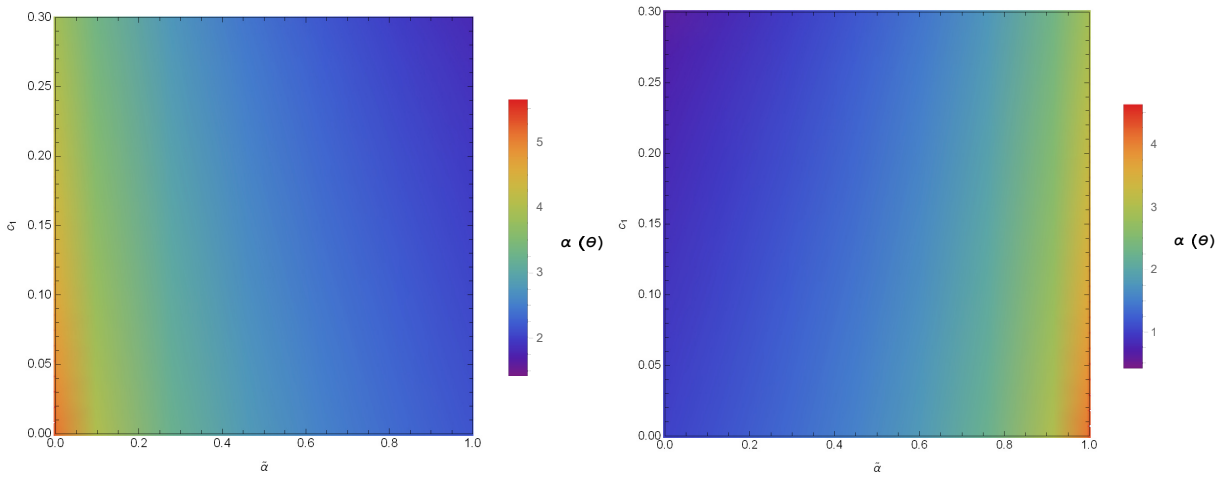

Figure 4. Color-indexed variations of the SD angle ($\alpha(\theta)$) with $\tilde{\alpha}$ and c_1 (**left**) for PPL and (**right**) for PPM. Here, we set $c_0 = \sqrt{3c_1 d + 1}$, $d = 1$, and $\Lambda = -1$.

5. Strong Deflection Gravitational Lensing Observables for *SgrA** and *M87**

To probe the polarization consequences for the photons in conformal gravity, we deal with the lens equation [28,126,127]:

$$\gamma = \frac{D_{OL} + D_{LS}}{D_{LS}}\theta - \alpha(\theta)\ mod\ 2\pi. \tag{39}$$

The variable γ represents the angle in the direction of the source, which is analogous to the optical axis, while D_{OL} stands for the observer lens distance and D_{LS} stands for the source lens distance. The angular separation s between the nth relativistic image and the lens yields the following result [28,126,127]:

$$\theta_n \simeq \theta_n^0 (1 - \frac{u_{ps} e_n (D_{OL} + D_{LS})}{\bar{a} D_{OL} D_{LS}}), \tag{40}$$

where

$$\theta_n^0 = (1 + e_n)\frac{u_{ps}}{D_{OL}}, \qquad e_n = e^{\frac{\bar{b} + |\gamma| - 2\pi n}{\bar{a}}}. \tag{41}$$

The position of the relativistic image analogous to the SD angle $\alpha(\theta) = 2n\pi$ for any number n is θ_n^0. The term $e_n \to 0$ (at $n \to \infty$) yields the impact parameter u_{ps} associated with an asymptotic position of the set of the images θ_∞:

$$u_{ps} = D_{OL}\theta_\infty\ . \tag{42}$$

Furthermore, to evaluate the coefficients ($\bar{a}$, $\bar{b}$) from Equation (37), we deal with the perfect situation [27,28,126,127], and hence we obtain the following relations:

$$s = \theta_1 - \theta_\infty = \theta_\infty e^{\frac{\bar{b} - 2\pi}{\bar{a}}}, \tag{43}$$

$$r = 2.5 \log R_0 = 2.5 \log(\frac{\mu_1}{\sum_{n=2}^{\infty} \mu_n}) = \frac{5\pi}{\bar{a}} \log e. \tag{44}$$

Here, the variable s stands for the angular separation, obtained by separating the outermost image (θ_1) and the innermost images (θ_∞). The variable r stands for the relative magnitudes, and the quantity R_0 stands for the flux ratio of the outermost image (θ_1) and the innermost images (θ_∞). With the help of these observables (θ_∞, s, and r), it is easy to evaluate the minimum impact parameter u_{ps} and the coefficients ($\bar{a}$, $\bar{b}$) of the SD angle in the conformal gravity black hole. We consider $SgrA^*$ to be a lens having a mass $M = 4.28 \times 10^6 M_\odot$ and $D_{OL} = 8.32$ kpc [123]. From this assumption, it is easy to estimate

the values of the observables (θ_∞, s, and r) for the SD gravitational lensing phenomenon. In general relativity, $SgrA^*$ is supposed to be a Schwarzschild black hole, and hence the values of the observables (θ_∞, s, and r) for the Schwarzschild black hole are $\theta_\infty = 26.4\ \mu as$, $s = 33.0\ nas$, and $r = 6.8\ mag$. The color-indexed values of the observables (θ_∞, s, and r) for the conformal gravity black hole are given in Figure 5, corresponding to the Schwarzschild black hole. Specifically, the observable θ_∞ varied, ranging from 15 μas to 45 μas for PPL and 14 μas to 43 μas for PPM, whereas it had the theoretically lower limits (i.e., when $c_1 = 0$ and $\tilde{\alpha} \to 0$) of 15 μas and 14 μas for PPL and PPM, respectively. Based on the results presented in Figure 5, the value of the observable s (angular separation) ranged from about 5 nanoarcseconds (nas) to about 35 nas for PPL, whereas the angular separation s ranged from about 7 nas to about 36 nas for PPM. In Figure 5, the observable r (relative magnitudes) had values ranging from 6 mag to 8.8 mag for PPL and from 5.3 mag to 8 mag for PPM. Similarly, these observables (θ_∞, s, and r) can easily be found by using the same technique for the case of $M87^*$ having a mass $m_\bullet = 6.5 \times 10^9 M_\odot$ and distance $D_{OL} = 16.9$ Mpc [124]. From Equations (42–44), we have the following relations for $M87^*$:

$$\begin{aligned} \theta_{\infty,M87^*} &= \frac{m_{\bullet,M87^*}}{m_{\bullet,SgrA^*}} \frac{D_{OL,SgrA^*}}{D_{OL,M87^*}} \theta_{\infty,SgrA^*} \\ &= 0.7484\ \theta_{\infty,SgrA^*}, \end{aligned} \tag{45}$$

$$s_{M87^*} = 0.7484\ s_{SgrA^*}, \tag{46}$$

$$r_{M87^*} = r_{SgrA^*}. \tag{47}$$

We assume $M87^*$ to be a Schwarzschild black hole. Then, the values of the observables θ_∞ and s for $M87^*$ are $\theta_\infty = 19.7\ \mu as$ and $s = 24.7\ nas$, whereas the observable $r = 6.8\ mag$ remains unchanged and obtains the same value as it attained in the case of $SgrA^*$. The pattern of the observables (θ_∞, s, and r) will be same in Figure 5, but their values will be changed for $M87^*$. We observed that the values of the observables θ_∞ and s for the conformal gravity black hole reached 11.25 μas for PPL, 11.48 μas for PPM as well as 26.194 nas for PPL and 26.942 nas for PPM, respectively. However, the observable r remained unchanged. It is viable to observe the quantum correction by calculating the variation of the shadow θ_∞ and the variations combined by the relativistic images, which are unworkable due to the lack of adequate angular separation. We have to assert repeatedly that being very accurate is a prerequisite when the calculation via EHT [128] is accurately practiced to constrain the conformal gravity BH considered here, as the models for measuring the properties of the shadow of $M87^*$ [124] obtain two essential factors: the rotation of the black hole and the GRMHD of the plasma about it, neither of which are studied in the present work. However, when placed on the calculated diameter $42 \pm 3\ \mu as$ of the shadow of $M87^*$ [128], we can measure the tentative and rough bounds on $\tilde{\alpha}$ and c_1 as $0.1 \leq \tilde{\alpha} \leq 1$ and $0.01 \leq c_1 \leq 0.3$ in the given domain $\mathcal{D}$. According to Figure 5, for $M87^*$, these are natural signs for the case of the quantum effect but not legitimate constraints on it. We would like to mention that $0.1 < \alpha < 1$ is a multiple of 10^{-7}.

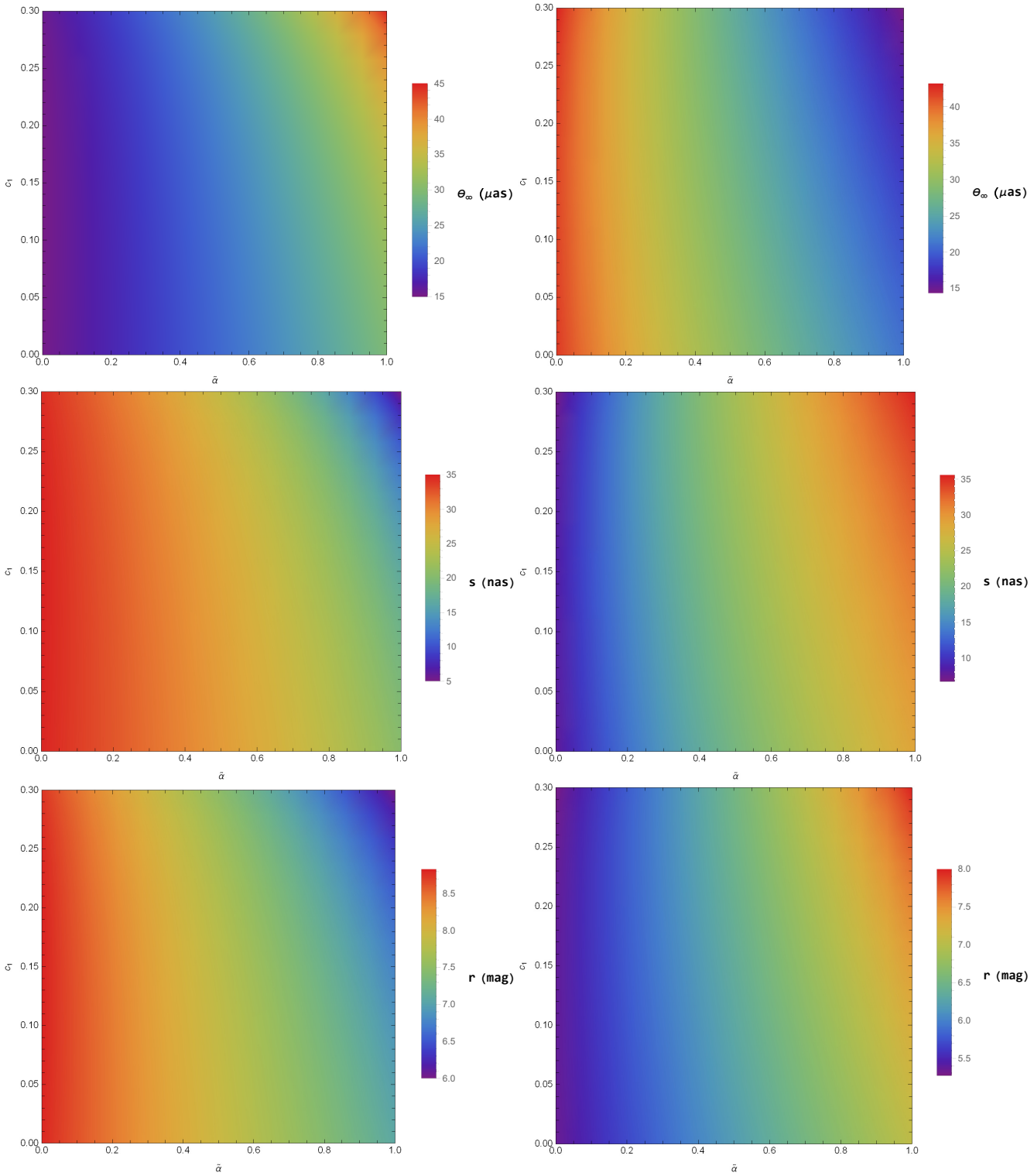

Figure 5. Color-indexed variations of the observables (θ_∞, s, and r) in the SD gravitational lensing in the conformal gravity BH from that of a Schwarzschild one for $SgrA^*$ (**left**) for PPL and (**right**) for PPM with $\tilde{\alpha}$ and c_1.

6. Conclusions

The SD gravitational lensing phenomenon and the dynamical equations of motion for photons were studied with the background of a conformal gravity black hole. We found that the black hole parameter c_1, the polarization directions, and the coupling parameter $\tilde{\alpha}$ are influential for the improvement of photons in the conformal gravity black hole. We

observed that the parameters played a significant role in expounding the photon sphere radius, the SD coefficients, the SD angle, and the other SD lensing observables. The altered light cone conditions recommend that the photons move along the null geodesics. We found that the photon sphere was described as the innermost circulating orbit for the photons, but the photon sphere radius was the largest root of Equation (26). In Figure 1, we presented the radius (x_{ps}) for the cases of PPL and PPM. This explains that with an increase in the coupling parameter and the constant c_1, the radius (x_{ps}) becomes $x_{ps} = 1.9$ and $x_{ps} = 2.85$ for PPL and PPM, respectively. The color-indexed deviations of the coefficients for the specific values of the constant c_1 were presented in Figures 2 and 3. We identified that the SD coefficients $\bar{a}$ and $\bar{b}$ had the values $\bar{a} = 1.25$ for PPL and $\bar{a} = 1$ for PPM, whereas $\bar{b} = 4.1$ for PPL and $\bar{b} = 3.2$ for PPM. The variation in the SD angle ($\alpha(\theta) = 5.75$ for PPL and $\alpha(\theta) = 4.75$ for PPM) was figured out to be $u = u_{ps} + 0.003$, as can be seen in Figure 4. By taking $SgrA^*$ and $M87^*$ as two lenses, it is concluded that the present technology can only calculate the supposed size of the shadows of black holes and their variations from those of the Schwarzschild type. On behalf of the calculated diameter of 42 ± 3 μas for $M87^*$'s shadow [128], we can have rough and tentative limits for the coupling parameter and the constant (c_1) as $0.1 \leq \tilde{\alpha} \leq 1$ and $0.01 \leq c_1 \leq 0.3$ in the given domain $\mathcal{D}$. According to Figure 5 (for $M87^*$), these are natural signs for the case of quantum effects but not legitimate conditions for it.

Author Contributions: Conceptualization, G.A. and A.Ö.; methodology, A.M.; software, M.Z.; validation, G.A. and A.Ö.; formal analysis, A.M.; investigation, A.M. and M.Z.; writing—original draft preparation, A.Ö.; writing—review and editing, G.A.; supervision, G.A. All authors have read and agreed to the published version of the manuscript.

Funding: This research received no external funding.

Data Availability Statement: Data used in this research is available from the corresponding author and will be provided on request.

Acknowledgments: A.Ö. would like to acknowledge the contribution of the COST Action CA18108-Quantum gravity phenomenology in the multi-messenger approach (QG-MM).

Conflicts of Interest: The authors declare no conflict of interest.

References

1. Adler, S.L. Einstein gravity as a symmetry-breaking effect in quantum field theory. *Rev. Mod. Phys.* **1982**, *54*, 729. [CrossRef]
2. Hooft, G.t. A class of elementary particle models without any adjustable real parameters. *arXiv* **2011**, arXiv:1104.4543.
3. Mannheim, P.D. Making the case for conformal gravity. *Found. Phys.* **2012**, *42*, 388. [CrossRef]
4. Bergshoeff, E.; de Roo, M.; Wit, B.d. Extended conformal supergravity. *Nucl. Phys. B* **1981**, *182*, 173. [CrossRef]
5. de Wit, B.; van Holten, J.W.; Proeyen, A.V. Structure of N = 2 supergravity. *Nucl. Phys. B* **1981**, *184*, 77. [CrossRef]
6. Berkovits, N.; Witten, E. Conformal supergravity in twistor-string theory. *J. High Energy Phys.* **2004**, *0408*, 009. [CrossRef]
7. Maldacena, J. Einstein Gravity from Conformal Gravity. *arXiv* **2011**, arXiv:1105.5632.
8. Anastasiou, G.; Olea, R. From conformal to Einstein gravity. *Phys. Rev. D* **2016**, *94*, 086008. [CrossRef]
9. Mannheim, P.D. Comprehensive solution to the cosmological constant, zero-point energy, and quantum gravity problems. *Gen. Rel. Grav.* **2011**, *43*, 703. [CrossRef]
10. Stelle, K.S. Renormalization of higher-derivative quantum gravity. *Phys. Rev. D* **1977**, *16*, 953. [CrossRef]
11. Mannheim, P.D.; Kazanas, D. Exact vacuum solution to conformal Weyl gravity and galactic rotation curves. *Astrophys. J.* **1989**, *342*, 635. [CrossRef]
12. Mannheim, P.D. Alternatives to dark matter and dark energy. *Prog. Part. Nucl. Phys.* **2006**, *56*, 340. [CrossRef]
13. Mannheim, P.D.; Brien, J.G.O. Impact of a global quadratic potential on galactic rotation curves. *Phys. Rev. Lett.* **2011**, *106*, 121101. [CrossRef]
14. Vagnozzi, S.; Roy, R.; Tsai, Y.D.; Visinelli, L.; Afrin, M.; Allahyari, A.; Bambhaniya, P.; Dey, D.; Ghosh, S.G.; Joshi, P.S.; et al. Horizon-scale tests of gravity theories and fundamental physics from the Event Horizon Telescope image of Sagittarius A*. *arXiv* **2022**, arXiv:2205.07787.
15. Lu, H.; Pang, Y.; Pope, C.N.; Vazquez-Poritz, J.F. AdS and Lifshitz black holes in conformal and Einstein-Weyl gravities. *Phys. Rev. D* **2012**, *86*, 044011. [CrossRef]
16. Xu, W.; Zhao, L. Critical phenomena of static charged AdS black holes in conformal gravity. *Phys. Lett. B* **2014**, *736*, 214. [CrossRef]

17. Xu, H.; Sun, Y.; Zhao, L. Black hole thermodynamics and heat engines in conformal gravity. *Int. J. Mod. Phys. D* **2017**, *26*, 1750151. [CrossRef]
18. Xu, H.; Yung, M.H. On the thermodynamic phase structure of conformal gravity. *Phys. Lett. B* **2018**, *783*, 36. [CrossRef]
19. Einstein, A. Lens-Like Action of a Star by the Deviation of Light in the Gravitational Field. *Science* **1936**, *84*, 2188, 506. [CrossRef]
20. Abbott, B.P.; Abbott, R.; Abbott, T.D.; Abernathy, M.R.; Acernese, F.; Ackley, K.; Adams, C.; Adams, T.; Addesso, P.; Adhikari, R.X.; et al. Observation of Gravitational Waves from a Binary Black Hole Merger. *Phys. Rev. Lett.* **2016**, *116*, 061102. [CrossRef]
21. Darwin, C. The gravity field of a particle. *Proc. R. Soc. Lond. A* **1959**, *249*, 180.
22. Virbhadra, K.S.; Ellis, G.F.R. Schwarzschild black hole lensing. *Phys. Rev. D* **2000**, *62*, 084003. [CrossRef]
23. Virbhadra, K.S.; Keeton, C.R. Time delay and magnification centroid due to gravitational lensing by black holes and naked singularities. *Phys. Rev. D* **2008**, *77*, 124014. [CrossRef]
24. Virbhadra, K.S. Relativistic images of Schwarzschild black hole lensing. *Phys. Rev. D* **2009**, *79*, 083004. [CrossRef]
25. Frittelly, S.; Kling, T.P.; Newman, E.T. Spacetime perspective of Schwarzschild lensing. *Phys. Rev. D* **2000**, *61*, 064021. [CrossRef]
26. Bozza, V.; Capozziello, S.; Lovane, G.; Scarpetta, G. Strong field limit of black hole gravitational lensing. *Gen. Rel. Grav.* **2001**, *33*, 1535. [CrossRef]
27. Bozza, V. Gravitational lensing in the strong field limit. *Phys. Rev. D* **2002**, *66*, 103001. [CrossRef]
28. Bozza, V. Quasiequatorial gravitational lensing by spinning black holes in the strong field limit. *Phys. Rev. D* **2003**, *67*, 103006. [CrossRef]
29. Wei, S.W.; Liu, Y.X.; Fu, C.E.; Yang, K.J. Strong field limit analysis of gravitational lensing in Kerr-Taub-NUT spacetime. *J. Cosmol. Astropart. Phys.* **2012**, *10*, 053. [CrossRef]
30. Wei, S.W.; Liu, Y.X. Equatorial and quasiequatorial gravitational lensingby a Kerr black hole pierced by a cosmic string. *Phys. Rev. D* **2012**, *85*, 064044. [CrossRef]
31. Kraniotis, G.V. Precise analytic treatment of Kerr and Kerr-(anti) de Sitter black holes as gravitational lenses. *Class. Quant. Grav.* **2011**, *28*, 085021. [CrossRef]
32. Eiroa, E.F.; Romero, G.E.; Torres, D.F. Reissner-Nordström black hole lensing. *Phys. Rev. D* **2002**, *66*, 024010. [CrossRef]
33. Eiroa, E.F. Gravitational lensing by Einstein-Born-Infeld black holes. *Phys. Rev. D* **2006**, *73*, 043002. [CrossRef]
34. Chen, S.B.; Jing, J.L. Strong field gravitational lensing in the deformed Hořava-Lifshitz black hole. *Phys. Rev. D* **2009**, *80*, 024036. [CrossRef]
35. Liu, Y.; Chen, S.B.; Jing, J.L. Strong gravitational lensing in a squashed Kaluza-Klein black hole spacetime. *Phys. Rev. D* **2010**, *81*, 124017. [CrossRef]
36. Chen, S.B.; Jing, J.L. Geodetic precession and strong gravitational lensing in dynamical Chern–Simons-modified gravity. *Class. Quantum Gravity* **2010**, *27*, 225006. [CrossRef]
37. Chen, S.B.; Liu, Y.; Jing, J.L. Strong gravitational lensing in a squashed Kaluza-Klein G$'$odel black hole. *Phys. Rev. D* **2011**, *83*, 124019. [CrossRef]
38. Ding, C.K.; Kang, S.; Chen, C.Y.; Chen, S.B.; Jing, J.L. Strong gravitational lensing in a noncommutative black-hole spacetime. *Phys. Rev. D* **2011**, *83*, 084005. [CrossRef]
39. Chen, S.B.; Jing, J.L. Strong gravitational lensing by a rotating non-Kerr compact object. *Phys. Rev. D* **2012**, *85*, 124029. [CrossRef]
40. Liu, C.Q.; Chen, S.B.; Jing, J.L. Strong gravitational lensing of quasi-Kerr compact object with arbitrary quadrupole moments. *J. High Energy Phys.* **2012**, *8*, 097. [CrossRef]
41. Ji, L.Y.; Chen, S.B.; Jing, J.L.J. Strong gravitational lensing in a rotating Kaluza-Klein black hole with squashed horizons. *J. High Energy Phys.* **2014**, 089. [CrossRef]
42. Zhang, R.J.; Jing, J.L.; Chen, S.B. Strong gravitational lensing for black holes with scalar charge in massive gravity. *Phys. Rev. D* **2017**, *95*, 064054. [CrossRef]
43. Drummond, I.T.; Hathrell, S.J. QED vacuum polarization in a background gravitational field and its effect on the velocity of photons. *Phys. Rev. D* **1980**, *22*, 343. [CrossRef]
44. Turner, M.S.; Widrow, L.M. Inflation-produced, large-scale magnetic fields. *Phys. Rev. D* **1988**, *37*, 2743. [CrossRef] [PubMed]
45. Ni, W.T. Equivalence Principles and Electromagnetism. *Phys. Rev. Lett.* **1977**, *38*, 301. [CrossRef]
46. Ni, W.T. Equivalence principles and precision experiments. In *Precision Measurements and Fundamental Constants II*; Taylor, B.N., Phillips, W.D., Eds.; U.S. National Bureau of Standards Publication 617; U.S. GPO: Washington, DC, USA, 1984.
47. Solanki, S.K.; Preuss, O.; Haugan, M.P.; Gandorfer, A.; Povel, H.P.; Steiner, P.; Stucki, K.; Bernasconi, P.N.; Soltau, D. Solar constraints on new couplings between electromagnetism and gravity. *Phys. Rev. D* **2004**, *69*, 062001. [CrossRef]
48. Preuss, O.; Haugan, M.P.; Solanki, S.K.; Jordan, S. An astronomical search for evidence of new physics: Limits on gravity-induced birefringence from the magnetic white dwarf RE J0317-853. *Phys. Rev. D* **2004**, *70*, 067101. [CrossRef]
49. Itin, Y.; Hehl, F.W. Maxwell's field coupled nonminimally to quadratic torsion: Axion and birefringence. *Phys. Rev. D* **2003**, *68*, 127701. [CrossRef]
50. Dereli, T.; Sert, O. Non-minimal $\ln(R)F^2$ couplings of electromagnetic fields to gravity: Static, spherically symmetric solutions. *Eur. Phys. J. C* **2011**, *71*, 1589. [CrossRef]
51. Balakin, A.B.; Lemos, J.P.S. Non-minimal coupling for the gravitational and electromagnetic fields: A general system of equations. *Class. Quantum Gravity* **2005**, *22*, 1867. [CrossRef]

52. Balakin, A.B.; Bochkarev, V.V.; Lemos, J.P.S. Nonminimal coupling for the gravitational and electromagnetic fields: Black hole solutions and solitons. *Phys. Rev. D* **2008**, *77*, 084013. [CrossRef]
53. Hehl, F.W.; Obukhov, Y.N. How does the electromagnetic field couple to gravity, in particular to metric, nonmetricity, torsion, and curvature? *Lect. Notes Phys.* **2001**, *562*, 479.
54. Mazzitelli, F.D.; Spedalieri, F.M. Scalar electrodynamics and primordial magnetic fields. *Phys. Rev. D* **1995**, *52*, 6694. [CrossRef]
55. Lambiase, G.; Prasanna, A.R. Gauge invariant wave equations in curved space-times and primordial magnetic fields. *Phys. Rev. D* **2004**, *70*, 063502. [CrossRef]
56. Raya, A.; Aguilar, J.E.M.; Bellini, M. Gravitoelectromagnetic inflation from a 5D vacuum state. *Phys. Lett. B* **2006**, *638*, 314. [CrossRef]
57. Campanelli, L.; Cea, P.; Fogli, G.L.; Tedesco, L. Inflation-produced magnetic fields in $R^n F^2$ and IF^2 models. *Phys. Rev. D* **2008**, *77*, 123002. [CrossRef]
58. Bamba, K.; Odintsov, S.D. Inflation and late-time cosmic acceleration in non-minimal Maxwell-$F(R)$ gravity and the generation of large-scale magnetic fields. *J. Cosmol. Astropart. Phys.* **2008**, *0804*, 024. [CrossRef]
59. Kim, K.T.; Kronberg, P.P.; Dewdney, P.E.; Landecker, T.L. The Halo and Magnetic Field of the Coma Cluster of Galaxies. *Astrophys. J.* **1990**, *355*, 29. [CrossRef]
60. Kim, K.T.; Tribble, P.C.; Kronberg, P.P. Detection of Excess Rotation Measure Due to Intracluster Magnetic Fields in Clusters of Galaxies. *Astrophys. J.* **1991**, *379*, 80. [CrossRef]
61. Clarke, T.E.; Kronberg, P.P.; Boehringer, H. A New Radio-X-Ray Probe of Galaxy Cluster Magnetic Fields. *Astrophys. J.* **2001**, *547*, L111. [CrossRef]
62. Ritz, A.; Ward, J. Weyl corrections to holographic conductivity. *Phys. Rev. D* **2009**, *79*, 066003. [CrossRef]
63. Wu, J.P.; Cao, Y.; Kuang, X.M.; Li, W.J. The 3+1 holographic superconductor with Weyl corrections. *Phys. Lett. B* **2011**, *697*, 153. [CrossRef]
64. Ma, D.Z.; Cao, Y.; Wu, J.P. The Stückelberg holographic superconductors with Weyl corrections. *Phys. Lett. B* **2011**, *704*, 604. [CrossRef]
65. Momeni, D.; Setare, M.R. A note on holographic superconductors with Weyl corrections. *Mod. Phys. Lett. A* **2011**, *26*, 2889. [CrossRef]
66. Momeni, D.; Majd, N.; Myrzakulov, R. p-Wave holographic superconductors with Weyl corrections. *Europhys. Lett.* **2012**, *97*, 61001.
67. Momeni, D.; Setare, M.R.; Myrzakulov, R. Condensation of the scalar field with Stuckelberg and Weyl corrections in the background of a planar AdS-Schwarzschild black hole. *Int. J. Mod. Phys. A* **2012**, *27*, 1250128. [CrossRef]
68. Roychowdhury, D. Effect of external magnetic field on holographic superconductors in presence of nonlinear corrections. *Phys. Rev. D* **2012**, *86*, 106009. [CrossRef]
69. Zhao, Z.X.; Pan, Q.Y.; Jing, J.L. Holographic insulator/superconductor phase transition with Weyl corrections. *Phys. Lett. B* **2013**, *719*, 440. [CrossRef]
70. Zhang, L.; Pan, Q.Y.; Jing, J.L. Holographic p-wave superconductor models with Weyl corrections. *Phys. Lett. B* **2015**, *743*, 104. [CrossRef]
71. Chen, S.B.; Jing, J.L. Dynamical evolution of the electromagnetic perturbation with Weyl corrections. *Phys. Rev. D* **2013**, *88*, 064058. [CrossRef]
72. Chen, S.B.; Jing, J.L. Dynamical evolution of a vector field perturbation coupled to the Einstein tensor. *Phys. Rev. D* **2014**, *90*, 124059. [CrossRef]
73. Liao, H.; Chen, S.B.; Jing, J.L. Absorption cross section and Hawking radiation of the electromagnetic field with Weyl corrections. *Phys. Lett. B* **2014**, *728*, 457. [CrossRef]
74. Jing, J.L.; Chen, S.B.; Pan, Q.Y. Geometric optics for a coupling model of electromagnetic and gravitational fields. *Ann. Phys.* **2016**, *367*, 219–226. [CrossRef]
75. Jing, J.L.; Chen, S.B.; Pan, Q.Y.; Wang, M.J. Detect black holes using photons for coupling model of electromagnetic and gravitational fields. *arXiv* **2017**, arXiv:1704.08794.
76. Chen, S.B.; Jing, J.L. Strong gravitational lensing for the photons coupled to Weyl tensor in a Schwarzschild black hole spacetime. *J. Cosmol. Astropart. Phys.* **2015**, *10*, 002. [CrossRef]
77. Cao, W.G.; Xie, Y. Weak deflection gravitational lensing for photons coupled to Weyl tensor in a Schwarzschild black hole. *Eur. Phys. J. C* **2018**, *78*, 191. [CrossRef]
78. Lu, X.; Yang, F.W.; Xie, Y. Strong gravitational field time delay for photons coupled to Weyl tensor in a Schwarzschild black hole. *Eur. Phys. J. C* **2016**, *76*, 357. [CrossRef]
79. Lu, X.; Xie, Y. Time delay of photons coupled to Weyl tensor in a regular phantom black hole. *Eur. Phys. J. C* **2020**, *80*, 625. [CrossRef]
80. Horvath, Z.; Gergely, L.A.; Keresztes, Z.; Harko, T.; Lobo, F.S.N. Constraining Hořava-Lifshitz gravity by weak and strong gravitational lensing. *Phys. Rev. D* **2011**, *84*, 083006. [CrossRef]
81. Eiroa, E.F.; Sendra, C.M. Gravitational lensing by massless braneworld black holes. *Phys. Rev. D* **2012**, *86*, 083009. [CrossRef]
82. Izmailov, R.N.; Karimov, R.K.; Zhdanov, E.R.; Nandi, K.K. Modified gravity black hole lensing observables in weak and strong field of gravity. *Mon. Not. Roy. Astron. Soc.* **2019**, *483*, 3754–3761. [CrossRef]

83. Gao, Y.X.; Xie, Y. Gravitational lensing by hairy black holes in Einstein-scalar-Gauss-Bonnet theories. *Phys. Rev. D* **2021**, *103*, 043008. [CrossRef]
84. Cheng, X.T.; Xie, Y. Probing a black-bounce, traversable wormhole with weak deflection gravitational lensing. *Phys. Rev. D* **2021**, *103*, 064040. [CrossRef]
85. Zhang, J.; Xie, Y. Gravitational lensing by a black-bounce-Reissner–Nordström spacetime. *Eur. Phys. J. C* **2022**, *82*, 471. [CrossRef]
86. Kuang, X.M.; Övgün, A. Strong gravitational lensing and shadow constraint from M87* of slowly rotating Kerr-like black hole. *Ann. Phys.* **2022**, *447*, 169147. [CrossRef]
87. Javed, W.; Atique, M.; Pantig, R.C.; Övgün, A. Weak Deflection Angle, Hawking Radiation and Greybody Bound of Reissner-Nordström Black Hole Corrected by Bounce Parameter. *Symmetry* **2023**, *15*, 148. [CrossRef]
88. Javed, W.; Riaz, S.; Pantig, R.C.; Övgün, A. Weak gravitational lensing in dark matter and plasma mediums for wormhole-like static aether solution. *Eur. Phys. J. C* **2022**, *82*, 1057. [CrossRef]
89. Javed, W.; Irshad, H.; Pantig, R.C.; Övgün, A. Weak Deflection Angle by Kalb–Ramond Traversable Wormhole in Plasma and Dark Matter Mediums. *Universe* **2022**, *8*, 599. [CrossRef]
90. Pantig, R.C.; Mastrototaro, L.; Lambiase, G.; Övgün, A. Shadow, lensing, quasinormal modes, greybody bounds and neutrino propagation by dyonic ModMax black holes. *Eur. Phys. J. C* **2022**, *82*, 1155. [CrossRef]
91. Pantig, R.C.; Övgün, A. Testing dynamical torsion effects on the charged black hole's shadow, deflection angle and greybody with M87* and Sgr. A* from EHT. *Ann. Phys.* **2023**, *448*, 169197. [CrossRef]
92. Uniyal, A.; Pantig, R.C.; Övgün, A. Probing a non-linear electrodynamics black hole with thin accretion disk, shadow, and deflection angle with M87* and Sgr A* from EHT. *Phys. Dark Univ.* **2023**, *40*, 101178. [CrossRef]
93. Jusufi, K.; Övgün, A. Gravitational Lensing by Rotating Wormholes. *Phys. Rev. D* **2018**, *97*, 024042. [CrossRef]
94. Övgün, A. Light deflection by Damour-Solodukhin wormholes and Gauss-Bonnet theorem. *Phys. Rev. D* **2018**, *98*, 044033. [CrossRef]
95. Pantig, R.C.; Övgün, A. Dark matter effect on the weak deflection angle by black holes at the center of Milky Way and M87 galaxies. *Eur. Phys. J. C* **2022**, *82*, 391. [CrossRef]
96. Li, G.; Deng, X.M. Classical tests of photons coupled to Weyl tensor in the Solar System. *Ann. Phys.* **2017**, *382*, 136. [CrossRef]
97. Li, G.; Deng, X.M. Testing Photons Coupled to Weyl Tensor with Gravitational Time Advancement. *Commun. Theor. Phys.* **2018**, *70*, 721. [CrossRef]
98. Pang, X.; Jia, J. Gravitational lensing of massive particles in Reissner–Nordström black hole spacetime. *Class. Quantum Gravity* **2019**, *36*, 065012. [CrossRef]
99. Tsukamoto, N. Deflection angle in the strong deflection limit in a general asymptotically flat, static, spherically symmetric spacetime. *Phys. Rev. D* **2017**, *95*, 064035. [CrossRef]
100. Zakharov, A.F.; de Paolis, F.; Ingrosso, G.; Nucita, A.A. Direct measurements of black hole charge with future astrometrical missions. *Astron. Astrophys.* **2005**, *442*, 795. [CrossRef]
101. Wang, C.Y.; Shen, Y.F.; Xie, Y. Weak and strong deflection gravitational lensings by a charged Horndeski black hole. *J. Cosmol. Astropart. Phys.* **2019**, *04*, 022. [CrossRef]
102. Lu, X.; Xie, Y. Weak and strong deflection gravitational lensing by a renormalization group improved Schwarzschild black hole. *Eur. Phys. J. C* **2019**, *79*, 1016. [CrossRef]
103. Whisker, R. Strong gravitational lensing by braneworld black holes. *Phys. Rev. D* **2005**, *71*, 064004. [CrossRef]
104. Zhao, S.S.; Xie, Y. Strong field gravitational lensing by a charged Galileon black hole. *J. Cosmol. Astropart. Phys.* **2016**, *07*, 007. [CrossRef]
105. Zhao, S.S.; Xie, Y. Strong deflection gravitational lensing by a modified Hayward black hole. *Eur. Phys. J. C* **2017**, *77*, 272. [CrossRef]
106. Chen, S.; Wang, S.; Huang, Y.; Jing, J.; Wang, S. Strong gravitational lensing for the photons coupled to a Weyl tensor in a Kerr black hole spacetime. *Phys. Rev. D* **2017**, *95*, 104017. [CrossRef]
107. Zhang, R.; Jing, J. Strong gravitational lensing for photons coupled to Weyl tensor in a regular phantom black hole. *Eur. Phys. J. C* **2018**, *78*, 796. [CrossRef]
108. Abbas, G.; Mahmood, A.; Zubair, M. Strong gravitational lensing for photon coupled to Weyl tensor in Kiselev black hole. *Chin. Phys. C* **2020**, *44*, 9. [CrossRef]
109. Abbas, G.; Mahmood, A.; Zubair, M. Strong deflection gravitational lensing for photon coupled to Weyl tensor in a charged Kiselev black hole. *Phys. Dark Universe* **2021**, *31*, 100750. [CrossRef]
110. Mannheim, P.D.; Kazanas, D. Current status of conformal Weyl gravity. *AIP Conf. Proc.* **1991**, *222*, 541.
111. Riegert, R.J. Birkhoff's Theorem in Conformal Gravity. *Phys. Rev. Lett.* **1984**, *53*, 315. [CrossRef]
112. Klemm, D. Topological black holes in Weyl conformal gravity. *Class. Quant. Grav.* **1998**, *15*, 3195. [CrossRef]
113. Hao, X.; Yung, M.-H. Black hole evaporation in conformal (Weyl) gravity. *Phys. Lett. B* **2019**, *793*, 97.
114. Daniels, R.D.; Shore, G.M. "Faster than light" photons and charged black holes. *Nucl. Phys. B* **1994**, *425*, 634. [CrossRef]
115. Daniels, R.D.; Shore, G.M. "Faster than light" photons and rotating black holes. *Phys. Lett. B* **1996**, *367*, 75. [CrossRef]
116. Shore, G.M. Faster than light photons in gravitational fields II.: Dispersion and vacuum polarisation. *Nucl.Phys. B* **2002**, *633*, 271. [CrossRef]
117. Cai, R.G. Propagation of vacuum polarized photons in topological black hole spacetimes. *Nucl. Phys. B* **1998**, *524*, 639. [CrossRef]

118. Cho, H.T. "Faster than light" photons in dilaton black hole spacetimes. *Phys. Rev. D* **1997**, *56*, 6416–6424. [CrossRef]
119. Lorenci, V.A.D.; Klippert, R.; Novello, M.; Salim, J.M. Light propagation in non-linear electrodynamics. *Phys. Lett. B* **2000**, *482*, 134. [CrossRef]
120. Breton, N. Geodesic structure of the Born–Infeld black hole. *Class. Quantum Grav.* **2002**, *19*, 601. [CrossRef]
121. Virbhadra, K.S.; Ellis, G.F.R. Gravitational lensing by naked singularities. *Phys. Rev. D* **2002**, *65*, 103004. [CrossRef]
122. Claudel, C.M.; Virbhadra, K.S.; Ellis, G.F.R. The geometry of photon surfaces. *J. Math. Phys.* **2001**, *42*, 818. [CrossRef]
123. Gillessen, S.; Plewa, P.M.; Eisenhauer, F.; Sari, R.; Waisberg, I.; Habibi, M.; Pfuhl, O.; George, E.; Dexter, J.; von Fellenberg, S.; et al. An Update on Monitoring Stellar Orbits in the Galactic Center. *Astrophys. J.* **2017**, *837*, 30. [CrossRef]
124. The Event Horizon Telescope Collaboration; Akiyama, K.; Alberdi, A.; Alef, W.; Asada, K.; Azulay, R.; Baczko, A.-K.; Ball, D.; Baloković, M.; Barrett, J.; et al. First M87 Event Horizon Telescope Results. VI. The Shadow and Mass of the Central Black Hole. *Astrophys. J. Lett.* **2019**, *875*, L6.
125. Virbhadra, K.S.; Narasimha, D.; Chitre, S.M. Role of the scalar field in gravitational lensing. *Astron. Astrophys.* **1998**, *337*, 1.
126. Bozza, V.; Luca, F.D.; Scarpetta, G.; Sereno, M. Analytic Kerr black hole lensing for equatorial observers in the strong deflection limit. *Phys. Rev. D* **2005**, *72*, 083003. [CrossRef]
127. Bozza, V.; Luca, F.D.; Scarpetta, G. Kerr black hole lensing for generic observers in the strong deflection limit. *Phys. Rev. D* **2006**, *74*, 063001. [CrossRef]
128. The Event Horizon Telescope Collaboration; Akiyama, K.; Alberdi, A.; Alef, W.; Asada, K.; Azulay, R.; Baczko, A.-K.; Ball, D.; Baloković, M.; Barrett, J.; et al. First M87 Event Horizon Telescope Results. I. The Shadow of the Supermassive Black Hole. *Astrophys. J. Lett.* **2019**, *875*, L1.

Disclaimer/Publisher's Note: The statements, opinions and data contained in all publications are solely those of the individual author(s) and contributor(s) and not of MDPI and/or the editor(s). MDPI and/or the editor(s) disclaim responsibility for any injury to people or property resulting from any ideas, methods, instructions or products referred to in the content.